Metal–Organic Supercontainers

DOI: 10.1002/anie.201406733

pH-Modulated Molecular Assemblies and Surface Properties of Metal–Organic Supercontainers at the Air–Water Interface**

Nathan L. Netzer, Feng-Rong Dai, Zhenqiang Wang, and Chaoyang Jiang**

Abstract: *The orientation of metal–organic supercontainer (MOSC) molecules in Langmuir films was systematically studied at the air–water interface. The acidity of the aqueous subphases plays a significant role in tuning the orientation of MOSC molecules in the Langmuir films. Furthermore, Langmuir–Blodgett films of MOSCs were prepared and the uniform multilayer structures demonstrated various surface properties, depending on their conditions of fabrication. Our use of Langmuir films provides a novel approach to access tunable assemblies of MOSC molecules in two-dimensional thin films.*

Over the past decade, framework-based porous solids, such as metal–organic frameworks (MOFs),[1] have been studied extensively as a result of their modular synthesis and exceptional performances in gas storage, separation, catalysis, and biomedical applications.[2] As a result of their polymeric framework structure, these materials typically exhibit negligible solubility in common solvents and investigations into their chemistry have been largely limited to the solid phase, often as bulk crystalline materials. Nevertheless, recent advances indicate that control of the size, shape, and morphology of MOF crystals in the nanoscale and mesoscale can lead to various dimensional structures that present unprecedented opportunities for functional applications.[3] Fabricating two-dimensional (2D) MOF structures, such as thin films, is of particular interest, as it readily affords material platforms that are desirable for use in devices for industrial applications, such as chemical sensing, catalysis, and membrane technologies.[4]

Several methods, such as layer-by-layer (LbL) assembly,[5] self-assembled monolayer (SAM) formation,[6] electrochemical deposition,[7] and the Langmuir–Blodgett (LB) technique,[8] have been utilized to study nanoscale structures and their 2D films. In nanofabrication, precise control and in situ characterization of molecular orientations and interactions are best governed by the LB technique.[9] For example, MOF LB films with unique structural characteristics, such as connected cavities and long-range crystalline orders, can be readily fabricated in situ through interfacial coordination reactions.[10] However, the poor solution processibility of MOFs means that MOF synthesis involving the assembly of soluble organic and inorganic precursors often has to be carried out as an integral part of the thin-film fabrication. This limitation presents several challenges including a lack of synthetic control and limited scope of the fabrication process.[10] In contrast, discrete metal–organic container structures show desirable solubility while retaining some key structural characteristics of MOFs,[11] and can afford new opportunities for thin-film fabrication. Recently, we reported a new family of nanoscale coordination container molecules, namely, metal–organic supercontainers (MOSCs), which can be assembled from divalent metal ions, carboxylate linkers, and sulfonylcalixarene-based container precursors.[12] MOSC molecules feature unusual multipore architectures, having both *endo* and *exo* cavities that are reminiscent of the structure of virus capsids,[13] and have shown great promise for designing novel porous functions because of their tunable "intrinsic" and "extrinsic" porosity.[14] Herein, we describe a direct and efficient approach to assembling MOSCs into two-dimensional thin films using the LB method. By separating the steps of material synthesis and thin-film fabrication, we can have more control on manipulating the structures of the thin films, making the fabrication process more generally applicable. Our goal was to demonstrate how the unique structural and solubility profiles of MOSCs may allow for facile fabrication of 2D thin films, and how the molecular orientations of MOSCs and surface properties of MOSC thin films can be systematically modulated by controlling the acidity of the aqueous subphases.

In the present study, we report intriguing results on the ability of a MOSC to preferentially orientate at the air–water interface as a function of subphase pH values. The molecular orientations of the MOSC molecules at the air–water interface were investigated by analyzing the surface pressure–molecular area (π–A) isotherms. This interfacial behavior, with respect to subphase pH values, was used to understand the anisotropic orientations of the MOSC molecule at the air–water interface. Furthermore, we studied the hydrophilicity of the MOSC LB films and found that the basic subphase generated a hydrophobic film, whereas an acidic or neutral subphase produced a hydrophilic film. Our results thus provide an in-depth understanding of the pH-modulated molecular orientation of MOSCs in LB films and helpful guidelines in designing novel 2D assemblies of container

[*] N. L. Netzer,[+] Dr. F. R. Dai,[+] Prof. Z. Wang, Prof. C. Jiang
Department of Chemistry
The University of South Dakota
414 E. Clark St., Vermillion, SD 57069 (USA)
E-mail: Zhenqiang.Wang@usd.edu
Chaoyang.Jiang@usd.edu

[+] These authors contributed equally to this work.

[**] This research was supported by the NSF (EPS-0903804 and DGE-0903685), NASA (Cooperative Agreement Number: NNX10AN34A), and by the state of South Dakota. A Langmuir–Blodgett trough was available through the US Department of Energy, contract number DE-EE0000270. Z.W. also acknowledges the support of an NSF CAREER Award (CHE-1352279). We thank Tam Ho for sample preparations and valuable discussions.

Supporting information for this article is available on the WWW under http://dx.doi.org/10.1002/anie.201406733.

molecules promising for a range of applications, such as selective guest adsorption and catalysis.[4a]

The MOSC chosen for this study, designated as **1-Co**, was synthesized as a crystalline material from the reaction of $Co(NO_3)_2{\cdot}6H_2O$, 1,4-benzenedicarboxylic acid (H_2BDC), and *p-tert*-butylsulfonylcalix[4]arene (H_4TBSC) in *N*,*N*-dimethyl-formamide (DMF) at 100 °C for 24 h, followed by the slow diffusion of diethyl ether or ethyl acetate into the reaction mixture.[12c] The structure and phase purity of **1-Co** were confirmed by a range of solid-state and solution techniques including X-ray diffraction, elemental analysis, and thermal gravimetric analysis. Elemental analysis revealed that the MOSC **1-Co** has an empirical formula of $[Co_4(\mu_4\text{-}H_2O)(TBSC)]_6(BDC)_{12}{\cdot}(DMF)_x{\cdot}(H_2O)_y$ ($x \approx 70$; $y \approx 90$) and a molecular topology of an edge-directed octahedron consisting of 24 Co^{II} ions, 6 TBSC units, and 12 BDC linkers (Scheme 1).[12c]

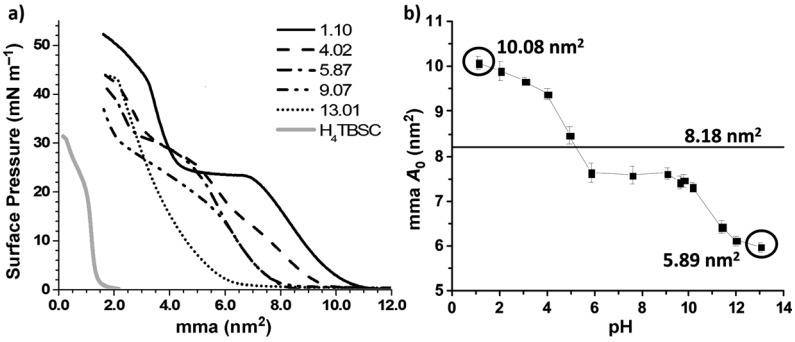

Figure 1. a) Langmuir isotherms of H_4TBSC on a neutral subphase (pH 5.9) and typical isotherms of **1-Co** on subphases at various pH values. b) The relationship between A_0 and subphase pH values, illustrating the decrease in A_0 value (molecular reorientation) as the pH value is increased.

Langmuir films of **1-Co** were prepared by initially dropping a chloroform solution of **1-Co** onto an air–water interface. After the evaporation of the chloroform, Langmuir films were compressed by two moving Teflon barriers and their phase behaviors were studied. Figure 1 a shows typical π–A isotherms of **1-Co** on subphases at various pH values, along with that of H_4TBSC on a neutral subphase with a pH of 5.9 (the neutral subphase has pH 5.9 because of dissolved CO_2). The isotherm of H_4TBSC shows typical behavior of fatty acid-like molecules with a small phase-transition at 20 mN m^{-1}.[15] A limiting area value (A_0) of the mean molecular areas (mma) is obtained at 1.4 nm^2, indicating a pinched-cone conformation of H_4TBSC at the air–water interface.[16] In contrast, the isotherms of **1-Co** display significantly different behavior. For the neutral subphase, the area of **1-Co** for pressure take-off is 7.63 nm^2, which is more than four times larger than that of H_4TBSC and can be attributed to the overall larger size of the MOSC molecule.

In addition to the variation in limiting area values between H_4TBSC and **1-Co** at pH 5.9, a pressure increase of the collapse point is evident, as well as a drastic increase in the length of the phase transition. Such differences confirm that the MOSC does not fragment into its calixarene precursor at the air–water interface. The obvious phase transition can be related to the possible orientation and configuration changes during the compress process, a behavior which has been previously observed.[15] For example, Merhi et al. proposed two types of molecular orientations for calixarene at the air–water interface: a parallel orientation where the lower rim of calixarene anchors into the subphase, and a second orientation where the calixarene cone is orientated perpendicularly to the subphase.[17] Similarly, various modes of MOSC molecular assemblies could exist during the monolayer compression at the air–water interface, as detailed below.

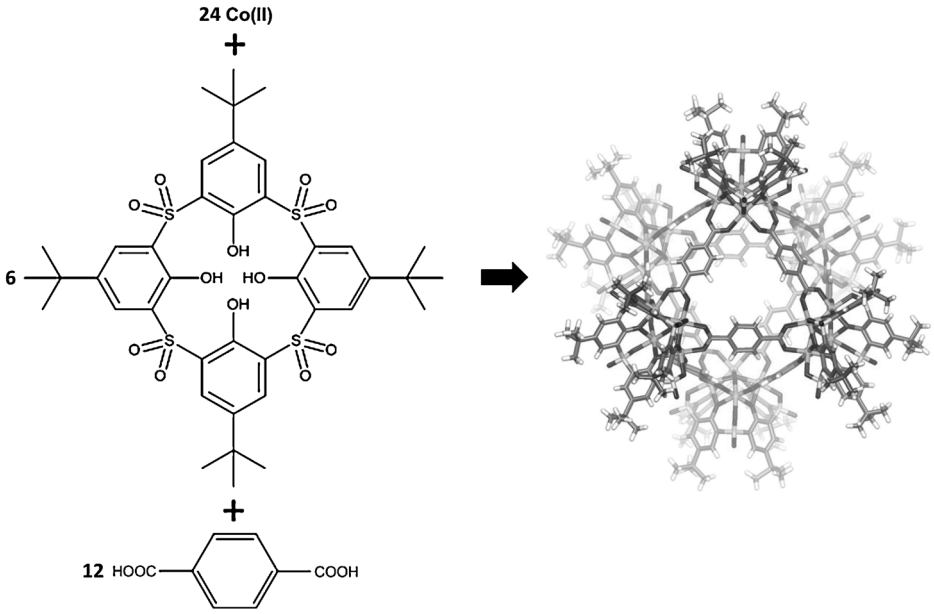

Scheme 1. Supramolecular assembly of the MOSC (**1-Co**) formed from a cobalt(II) salt, H_4TBSC, and H_2BDC.

Figure 1 a also shows selected π–A isotherms of **1-Co** with substrates at different pH values (see Figure S1 in the Supporting Information for full experimental data). Altering the subphase pH value caused noticeable changes in two aspects of the isotherms, specifically, the length of the phase transition and mean molecular areas. The phase transition state at approximately 25 mN m^{-1} is drastically different between the acidic and basic conditions. A large phase transition or compression plateau occurs under acidic conditions, whereas little to no phase transition is detected under basic conditions. The

absence of configuration change (i.e., a phase transition) for monolayers at high subphase pH values suggests that **1-Co** molecules most likely have different packing modes compared with the acidic subphase and that the monolayers are less compressible. In other words, compared to the basic conditions, **1-Co** undergoes more configurational changes to reach its final packing arrangement when interacting with acidic subphases.

The change of the mma value with respect to the pH values of subphases is clearly indicated in Figure 1b. A gradual transition of A_0 values is evident from 10.08 to 5.89 nm^2: the largest A_0 values are calculated for MOSC monolayers on the acidic subphases, a neutral subphase gives an intermediate mma value (7.6 nm^2), and the MOSC monolayers express the smallest A_0 values on the basic subphases. It should be noted that the dotted line at 8.18 nm^2 in Figure 1b shows the projected area along the *c*-axis for **1-Co** molecules based on the single-crystal XRD data (Figure S2).[12c] We attribute the change in A_0 values to the variation of intermolecular interactions between **1-Co** molecules, which are associated through intermolecular noncovalent forces such as ionic, van der Waals, and hydrophobic interactions. These interactions can play critical roles in determining the final packing structure of the 2D monolayer films at the air–water interface.[15,16,18] Based on the crystal structure, we propose possible orientations that **1-Co** may exhibit when suspended on an acidic or basic subphase (Figure 2). Although **1-Co** is

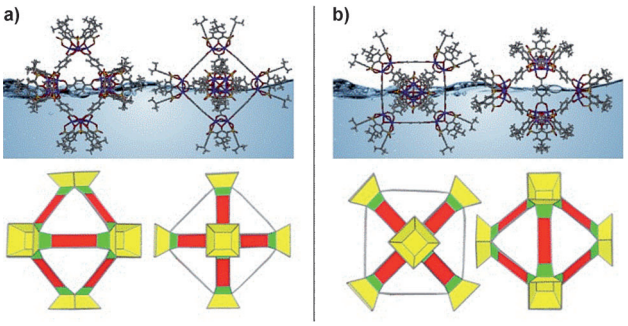

Figure 2. Cross-sectional view of the predicted **1-Co** molecular orientations at the air–water interface under a) acidic and b) basic subphase conditions.

a neutral compound in its as-synthesized form,[12c] the molecules may have become partially protonated under acidic subphase conditions at either the coordinating carboxylate or μ_4-O sites.[19] As a result of the stronger charge repulsion, the resulting cationic molecules likely adopt a highly open packing structure at the air–water interface that can be approximately described as primitive cubic packing, in which the TBSC units from adjacent **1-Co** molecules have a relatively long-range association with each other in a head-to-head fashion (Figure 2a). As a result of such non-close packing, large mma values are calculated under acidic conditions.

In contrast, for subphases with pH values within the range pH = 6–9, **1-Co** remains as a neutral compound as protonation does not take place under these conditions. The molecules likely retain the same body-centered cubic (bcc) packing seen in its crystal structure,[12c] as indicated by the corresponding mma values which closely resemble those derived from the X-ray structural analysis (Figure 1b). Intriguingly, under basic conditions, **1-Co** molecules seem to favor a closer packing arrangement between the calixarene moieties at the air–water interface, leading to mma values significantly smaller than the 8.18 nm^2 mark calculated from the bcc-type crystal structure (Figure 1b). We attribute this interesting finding to the tendency of the TBSC units from one MOSC molecule to orientate deeper inside the surface of a neighboring one through closer contact with the face of the octahedron (Figure 2b). To a certain extent, the transition from a relatively open structure under acidic or neutral conditions to a close packing mode under basic conditions at the air–water interface is reminiscent of the partial structural collapse that we recently demonstrated of **1-Co** solids upon solvent evacuation.[12c] Although the exact mechanism accounting for the close packing mode of **1-Co** under basic conditions remains unclear, it is believed that the molecule's enhanced hydrophobicity is the main driving force.

The molecular assemblies of **1-Co** molecules were further investigated after the Langmuir monolayer was transferred onto a glass substrate to form a LB film.[20] Herein, the uniformity of multilayer LB films was studied by measuring their UV/Vis absorption spectra. Figure 3a shows the UV/Vis absorption spectra of basic **1-Co** LB films containing one, three, five, and seven layers, respectively. It is noteworthy that the **1-Co** LB films have similar absorption bands as compared to their solution spectra (Figure 3b), corroborating the structural integrity of the MOSC molecules at the water–air interface. The inset of Figure 3a shows the linear relationships between the absorption intensity (at $\lambda = 227$ and 350 nm) and the number of LB layers, which confirms the uniform deposition of the MOSC LB films.

We envisioned that this ability to manipulate the molecular orientations and supramolecular assemblies of MOSC molecules at the air–water interface should allow us to design tunable surface properties for the fabricated LB films. To this end, we performed contact angle measurements for the **1-Co** LB films that were prepared with acidic (pH 2.0), neutral (pH 5.9), and basic (pH 10.9) subphases, respectively. As shown in Figure 3c, the acidic and neutral LB films express a hydrophilic behavior with contact angles below 20°, whereas the basic LB film gives a contact angle of 80°. The hydrophilic nature of **1-Co** LB films at acidic and neutral conditions can be ascribed to the supposedly lower density of calixarene cones on the surface of the LB films (Figure 2a), as well as the partial protonation of **1-Co** molecules in the case of acidic subphases. This is consistent with the results obtained from the π–A isotherms, where protonation of **1-Co** molecules under acidic conditions generated cationic compounds that experience strong electrostatic repulsion. It is worth noting that preliminary results also suggest that the MOSC-based LB films can adsorb dye molecules (e.g., methylene blue) in a manner similar to the bulk crystalline material (Figure S3), indicating that the nanoscale porosity of the MOSC is not compromised as a result of the 2D fabrication. That the modulation of molecular orientation and surface hydrophilicity of MOSC LB films can be achieved by simply adjusting

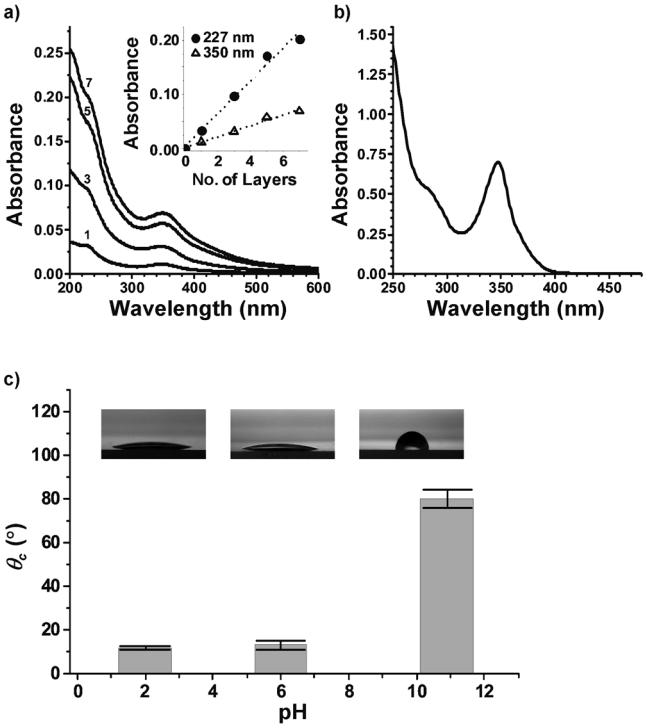

Figure 3. a) UV/Vis absorption spectra of multilayered basic LB films. Inset: linear absorbance of $\lambda = 350$ nm and 227 nm UV/Vis absorption bands. b) UV/Vis absorption spectrum of **1-Co** in a chloroform solution. c) Contact angles of the **1-Co** LB films (inset = photographs of the contact angle results).

the pH values of the subphase underlines the most appealing elements of our approach: it is highly efficient, has a high degree of synthetic control, and may lead to functional properties not directly accessible in bulk materials. Future work will involve a detailed structural study on **1-Co** LB films which will be carried out using a small-angle X-ray scattering technique. We further contemplate that three key characteristics, specifically solution processibility, chemical robustness, and structural/compositional versatility and tunability, contribute to the successful preparation of our MOSC LB films. As many other molecular containers also have such attributes, we anticipate our approach to be a generally applicable method.

In summary, we have shown that Langmuir–Blodgett assembly can be an effective method for preparing two-dimensional MOSC thin films. The orientation of **1-Co** at the air–water interface is highly dependent on the acidity of the subphase. Various surface hydrophilicities of MOSC LB films were observed because of the changes of molecular orientations in the LB films. The ability to assemble pH responsive MOSCs in various configurations opens a new avenue to tune the properties of container molecules in two-dimensional thin films, thus potentially allowing new functionality for such novel materials. In addition, utilizing the LB technique to study 2D films of container molecules affords a better understanding of the behavior of container molecules and their assemblies, thus facilitating their potential applications in a variety of areas including selective adsorption and catalysis.

Experimental Section

Deionized (DI) water (18.2 MΩ-cm) was obtained from a Barnstead diamond nanopure system. H_2SO_4 and H_2O_2 were purchased from Fisher. Chloroform (99.9%) was purchased from Acros. Optical grade quartz slides were purchased from AdValue Technology and rendered hydrophilic with a piranha solution (3:1, H_2SO_4:H_2O_2). Langmuir monolayers are prepared with a KSV 2000 LB trough. The pH values of the subphases are adjusted by NaOH or HCl and measured with an Accumet AR10 pH meter. A $CHCl_3$ solution of **1-Co** (350 μL) was spread drop-wise on the subphase surface (780 cm^2) and the solvent was allowed to fully evaporate. Then the monolayer was compressed at 10 $mm^2 min^{-1}$ to measure the π–A isotherms. To prepare multilayer LB films, the Langmuir layers were transferred to a pre-treated hydrophilic quartz substrate using a robotic dipper (2 $mm\,min^{-1}$) at designed surface pressure. The LB films were then fully dried before any further characterization.

Received: June 30, 2014
Revised: July 23, 2014
Published online: August 25, 2014

Keywords: coordination containers · Langmuir–Blodgett films · microporous materials · molecular orientation · supramolecular chemistry

[1] H.-C. Zhou, J. R. Long, O. M. Yaghi, *Chem. Rev.* **2012**, *112*, 673 – 674.
[2] a) M. P. Suh, H. J. Park, T. K. Prasad, D. W. Lim, *Chem. Rev.* **2012**, *112*, 782 – 835; b) J. R. Li, J. Sculley, H. C. Zhou, *Chem. Rev.* **2012**, *112*, 869 – 932; c) W. M. Bloch, R. Babarao, M. R. Hill, C. J. Doonan, C. J. Sumby, *J. Am. Chem. Soc.* **2013**, *135*, 10441 – 10448; d) T. Li, J. E. Sullivan, N. L. Rosi, *J. Am. Chem. Soc.* **2013**, *135*, 9984 – 9987; e) M. Yoon, R. Srirambalaji, K. Kim, *Chem. Rev.* **2012**, *112*, 1196 – 1231; f) M. Zhao, S. Ou, C. D. Wu, *Acc. Chem. Res.* **2014**, *47*, 1199 – 1207; g) P. Horcajada, R. Gref, T. Baati, P. K. Allan, G. Maurin, P. Couvreur, G. Ferey, R. E. Morris, C. Serre, *Chem. Rev.* **2012**, *112*, 1232 – 1268; h) A. Foucault-Collet, K. A. Gogick, K. A. White, S. Villette, A. Pallier, G. Collet, C. Kieda, T. Li, S. J. Geib, N. L. Rosi, S. Petoud, *Proc. Natl. Acad. Sci. USA* **2013**, *110*, 17199 – 17204.
[3] a) T. Li, M. T. Kozlowski, E. A. Doud, M. N. Blakely, N. L. Rosi, *J. Am. Chem. Soc.* **2013**, *135*, 11688 – 11691; b) S. Furukawa, J. Reboul, S. Diring, K. Sumida, S. Kitagawa, *Chem. Soc. Rev.* **2014**, *43*, 5700 – 5734.
[4] a) A. Bétard, R. A. Fischer, *Chem. Rev.* **2012**, *112*, 1055 – 1083; b) O. Shekhah, J. Liu, R. A. Fischer, C. Woll, *Chem. Soc. Rev.* **2011**, *40*, 1081 – 1106; c) B. Liu, O. Shekhah, H. K. Arslan, J. Liu, C. Wöll, R. A. Fischer, *Angew. Chem. Int. Ed.* **2012**, *51*, 807 – 810; *Angew. Chem.* **2012**, *124*, 831 – 835; d) G. Xu, T. Yamada, K. Otsubo, S. Sakaida, H. Kitagawa, *J. Am. Chem. Soc.* **2012**, *134*, 16524 – 16527.
[5] Y. Bao, Q. A. N. Luu, C. K. Lin, J. M. Schloss, P. S. May, C. Y. Jiang, *J. Mater. Chem.* **2010**, *20*, 8356 – 8361.
[6] K. P. Browne, B. A. Grzybowski, *Langmuir* **2011**, *27*, 1246 – 1250.
[7] C. R. Wade, M. Li, M. Dincă, *Angew. Chem. Int. Ed.* **2013**, *52*, 13377 – 13381; *Angew. Chem.* **2013**, *125*, 13619 – 13623.
[8] J. Y. Park, R. C. Advincula, *Soft Matter* **2011**, *7*, 9829 – 9843.
[9] a) S. Acharya, J. P. Hill, K. Ariga, *Adv. Mater.* **2009**, *21*, 2959 – 2981; b) J. A. Kitchen, D. E. Barry, L. Mercs, M. Albrecht, R. D. Peacock, T. Gunnlaugsson, *Angew. Chem. Int. Ed.* **2012**, *51*, 704 – 708; *Angew. Chem.* **2012**, *124*, 728 – 732.
[10] a) R. Makiura, S. Motoyama, Y. Umemura, H. Yamanaka, O. Sakata, H. Kitagawa, *Nat. Mater.* **2010**, *9*, 565 – 571; b) R. Makiura, K. Tsuchiyama, O. Sakata, *CrystEngComm* **2011**, *13*, 5538 – 5541; c) S. Motoyama, R. Makiura, O. Sakata, H. Kita-

gawa, *J. Am. Chem. Soc.* **2011**, *133*, 5640 – 5643; d) R. Makiura, O. Konovalov, *Sci. Rep.* **2013**, *3*, 2506; e) K. Hoshiko, T. Kambe, R. Sakamoto, K. Takada, H. Nishihara, *Chem. Lett.* **2014**, *43*, 252 – 253; f) R. Makiura, O. Konovalov, *Dalton Trans.* **2013**, *42*, 15931 – 15936.

[11] a) M. Yoshizawa, J. K. Klosterman, M. Fujita, *Angew. Chem. Int. Ed.* **2009**, *48*, 3418 – 3438; *Angew. Chem.* **2009**, *121*, 3470 – 3490; b) D. L. Caulder, K. N. Raymond, *Acc. Chem. Res.* **1999**, *32*, 975 – 982; c) R. Chakrabarty, P. S. Mukherjee, P. J. Stang, *Chem. Rev.* **2011**, *111*, 6810 – 6918; d) S. J. Dalgarno, N. P. Power, J. L. Atwood, *Coord. Chem. Rev.* **2008**, *252*, 825 – 841; e) M. M. J. Smulders, I. A. Riddell, C. Browne, J. R. Nitschke, *Chem. Soc. Rev.* **2013**, *42*, 1728 – 1754.

[12] a) F.-R. Dai, Z. Wang, *J. Am. Chem. Soc.* **2012**, *134*, 8002 – 8005; b) F.-R. Dai, D. C. Becht, Z. Wang, *Chem. Commun.* **2014**, *50*, 5385 – 5387; c) F.-R. Dai, U. Sambasivam, A. J. Hammerstrom, Z. Wang, *J. Am. Chem. Soc.* **2014**, *136*, 7480 – 7491.

[13] M. G. Mateu, *Structure and Physics of Viruses: An Integrated Textbook*, Springer, Heidelberg, **2013**.

[14] J. T. A. Jones, T. Hasell, X. F. Wu, J. Bacsa, K. E. Jelfs, M. Schmidtmann, S. Y. Chong, D. J. Adams, A. Trewin, F. Schiffman, F. Cora, B. Slater, A. Steiner, G. M. Day, A. I. Cooper, *Nature* **2011**, *474*, 367 – 371.

[15] L. Dei, A. Casnati, P. Lonostro, P. Baglioni, *Langmuir* **1995**, *11*, 1268 – 1272.

[16] F. Wang, X. Z. Jiang, L. Gao, L. T. Zhao, *J. Chin. Chem. Soc.* **2013**, *60*, 185 – 190.

[17] G. Merhi, M. Munoz, A. W. Coleman, G. Barrat, *Supramol. Chem.* **1995**, *5*, 173 – 177.

[18] X. L. Wu, P. L. Luo, S. J. Zhu, S. S. Zhang, B. X. Ye, *J. Chin. Chem. Soc.* **2011**, *58*, 362 – 368.

[19] T. Kajiwara, T. Kobashi, R. Shinagawa, T. Ito, S. Takaishi, M. Yamashita, N. Iki, *Eur. J. Inorg. Chem.* **2006**, 1765 – 1770.

[20] A. R. Tao, J. X. Huang, P. D. Yang, *Acc. Chem. Res.* **2008**, *41*, 1662 – 1673.

